*Proc. Natl. Acad. Sci. USA*
Vol. 87, pp. 7453–7456, October 1990
Biophysics

# Contraction of myofibrils in the presence of antibodies to myosin subfragment 2

**(force production in muscle/muscle contraction/shortening of myofibrils)**

WILLIAM F. HARRINGTON*, TRUDY KARR*, WILLIAM B. BUSA*, AND STEPHEN J. LOVELL†

*Department of Biology, Johns Hopkins University, Baltimore, MD 21218; and †Becton Dickinson, Advanced Diagnostics Division, 1400 Coppermine Terrace, Baltimore, MD 21209

*Contributed by William F. Harrington, July 20, 1990*

ABSTRACT **In a muscle-based version of *in vitro* motility assays, the unloaded shortening velocity of rabbit skeletal myofibrils has been determined in the presence and absence of affinity-column-purified polyclonal antibodies directed against the subfragment-2 region of myosin. Contraction was initiated by photohydrolysis of caged ATP and the time dependence of shortening was monitored by an inverted microscope equipped with a video camera. Antibody-treated myofibrils undergo unloaded shortening in a fast phase with initial rates and half-times comparable to control (untreated) myofibrils, despite a marked reduction in the isometric force of skinned muscle fibers in the presence of the antibodies. In antibody-treated myofibrils, this process is followed by a much slower phase of contraction, terminating in elongated structures with well-defined sarcomere spacings (≈1 μm) in contrast to the supercontracted globular state of control myofibrils. These results suggest that although the unloaded shortening of myofibrils (and *in vitro* motility of actin filaments over immobilized myosin heads) can be powered by myosin heads, the subfragment-2 region as well as the myosin head contributes to force production in actively contracting muscle.**

The classical rotating cross-bridge model proposes that the contractile force in activated muscle originates from a structural transition within the myosin head [subfragment-1 (S-1) subunit] while it is attached to actin (1, 2). The helix-coil model proposes that melting within subfragment-2 (S-2; the α-helical tail segment of heavy meromyosin) is triggered and generates force when the actin-attached cross-bridge swings away from the thick filament surface (3, 4). In earlier work (5), it was shown that purified anti-S-2 antibody can markedly depress the isometric tension generated by skinned psoas fibers. The reduction in tension (to about 7% of control fibers) occurs in the absence of any direct effect on the ability of S-1 to undergo cyclic interaction with actin as measured by the ATPase of antibody-treated fibers. One interpretation of this experiment is that S-2 contributes to force production *in vivo*, possibly through a helix-coil transition in the S-2 hinge domain of the myosin molecule (for review, see ref. 6). However, it seems clear from recent *in vitro* model studies that S-1 alone, energized by ATP, can produce force (7) and slide actin filaments at speeds approaching those obtained with muscle fibers under no-load conditions (8, 9). One possibility to reconcile these observations is that the force generated by S-1 in the model systems is sufficient to produce sliding motion but not sufficient for the expression of the full isometric force developed in working muscle. To test this explanation, we have measured the relative unloaded sliding velocity of overlapping thin and thick filaments in myofibrils, the intact basic structural units of skeletal muscle, in the presence and absence of polyclonal antibodies directed against the S-2 region of myosin. In these experiments, we have employed a methodology developed to monitor rapid changes in myofibrillar structure after initiation of contraction by photoactivation of caged ATP. We show below that antibody-treated myofibrils contract at a rate similar to that of untreated myofibrils. Thus, despite the severe drop in isometric force in antibody-treated fibers, the sliding process between thick and thin filaments in myofibrils seems to be relatively unimpaired. This suggests that the S-2 segment as well as the S-1 subunit contribute to active force in working muscle, but S-1 alone may be sufficient to support the unloaded shortening of myofibrils.

The publication costs of this article were defrayed in part by page charge payment. This article must therefore be hereby marked "*advertisement*" in accordance with 18 U.S.C. §1734 solely to indicate this fact.

## MATERIALS AND METHODS

Myofibrils were incubated at 4°C overnight in rigor buffer in the presence or absence of antibody (3 mg/ml). Rigor buffer (10) is 30 mM Pipes/3.1 mM $MgCl_2$/20 mM $CaCl_2$/20 mM EGTA/10.5 mM creatine phosphate/20 mM glutathione, pH 7.3. Before activation, myofibrils were mixed with an equivalent volume of rigor buffer containing caged ATP (20 mM) and creatine phosphokinase (100 units/ml), which had been treated with apyrase to remove any trace of free ATP. The apyrase was separated from the caged ATP solution by filtration through a Centricon-10 microconcentrator (5000 × *g* for 1.5 hr).

A 2.5- to 5-μl drop of activating solution containing myofibrils was placed between two coverslips for photoactivation. Before use, coverslips were soaked in Micro laboratory cleaning solution (International Products, Trenton, NJ) and then in 20 mM EGTA/10 mM Pipes, pH 7.5, for 1 hr. After thorough rinsing and drying (200°C), they were treated with a siliconizing agent (SurfaSil; Pierce) to reduce adhesion of myofibrils. SurfaSil (5 μl) was placed on a large (22 × 60 mm) lower coverslip or 2.5 μl was placed on the upper coverslip (22 × 22 mm) and the two surfaces were polished exhaustively with a Kimwipe.

**Data Collection.** Caged ATP (11) in the activating solution was conveniently photohydrolyzed on the microscope stage without recourse to specialized equipment, such as flashlamps or lasers, by taking advantage of the UV-transmitting optical path of the standard Nikon Diaphot inverted microscope. An uncased 25-mm aperture electronic shutter with gold-coated leaves (Uniblitz) was interposed between the field lens and the filter cube housing of the epifluorescence attachment. The shutter was controlled by a Uniblitz model 100-2B controller triggered by signals from the imaging computer. The filter cube (designed for use with the fluorescent dye fura-2) contained a Nikon DM400 dichroic mirror (cut-on at 325 nm and cut-off at 400 nm) and BA510 barrier filter; no excitation filter was used. The objective was a Nikon UV Fluor DL ×40. The UV source was a 75-W xenon

Abbreviations: S-1 and S-2, subfragment-1 and subfragment-2, respectively.

arc lamp housed in a standard Nikon epi-illuminator. The transillumination pathway (visible light) contained a green interference filter. Visible light images formed by the microscope were directed to a Dage CCD camera at the camera port of the microscope.

To initiate caged ATP hydrolysis and myofibril contraction, an 8-msec signal was sent from the imaging computer to the shutter controller. We used the ASCII "null" character sent through the computer's serial port at 1200 baud as a control signal, thus achieving a shutter open time and UV exposure of about 8 msec. In preliminary experiments, longer UV exposures did not alter the results reported here but made it difficult to observe the initial rate of contraction; exposures shorter than 8 msec were not feasible with the simple system described here. Simultaneous with the shutter control signal, the imaging computer (a Sun 3/110 workstation with a Datacube Minvideo board running IC200 imaging software from Inovision Corp., Research Triangle Park, NC) commenced storing to memory sequential video images of the preparation at a rate of 15–30 frames per sec. These image sequences were later written to digital tape off-line. Rates of myofibril contraction were determined off-line with the aid of the IC200 and custom software. For each sequential video frame the ends of myofibrils or sarcomeres were empirically selected using a "mouse," and the distance between these points was calculated by the computer.

**Data Analysis.** Average sarcomere spacing was determined by measuring the end-to-end length of a myofibril divided by the number of sarcomeres before activation. The average sarcomere length at each time point after the light pulse was calculated from the end-to-end length. This procedure allowed us to follow the shortening process throughout the early and late phases of the contraction when the sarcomere spacing of the control myofibrils became blurred and indistinct. We found no measurable difference in average sarcomere spacing by using this procedure and by direct measurement of sarcomere spacing during the early phase of contraction. The resulting data were averaged at each time point and the overall process in the fast phase was fitted (12) using a single exponential function (solid lines in Fig. 1).

**Preparation of Antibodies.** Polyclonal antibodies against the S-2 region of chicken pectoralis myosin produced in rabbit (rabbit anti-chicken S-2) and polyclonal antibodies against the S-2 region of rabbit psoas myosin produced in goat (goat anti-rabbit S-2) were prepared and purified as described (5). Rabbit myosin S-2 was isolated (13) and further purified by calcium precipitation (5).

**Preparation of Single Fibers, Myofibrils, and the Measurement of Isometric Force.** These procedures have been described in ref. 14.

## RESULTS

Two affinity-column-purified anti-S-2 antibodies were used in these experiments, polyclonal rabbit anti-chicken S-2 antibodies against the S-2 region of chicken pectoralis myosin and polyclonal goat anti-rabbit S-2 antibodies against the S-2 region of rabbit skeletal myosin.

Fig. 1 compares the rates of active shortening of rabbit psoas myofibrils that had been incubated overnight in rigor buffer in the presence and absence of the two antibodies. Contraction was initiated by photoactivation of caged ATP (8-msec flash) and followed using an inverted microscope equipped with a video camera. Ordinate values are average sarcomere spacings taken at equivalent times from experiments on two preparations of myofibrils. The sarcomere length vs. time profiles are qualitatively similar in the presence and absence of antibody. They show a rapid contraction from the original rigor lengths of ≈2.7 μm, which is complete in 400–700 msec. In the untreated myofibrils, this phase is

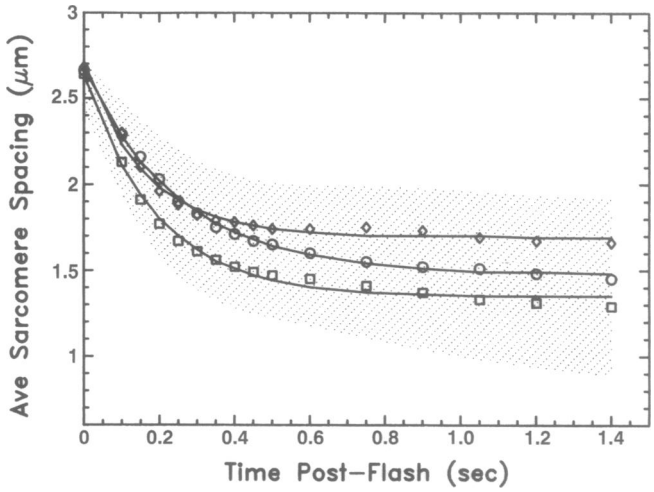


FIG. 1. Average sarcomere spacing vs. time of activated rabbit psoas myofibrils. Activation was initiated by photohydrolysis of caged ATP (8 msec per flash). □, Control (untreated) myofibrils; ◇, myofibrils in presence of polyclonal goat anti-rabbit S-2 antibody (IgG) against long S-2 region of rabbit psoas myosin; ○, myofibrils in presence of polyclonal rabbit anti-chicken S-2 antibody (IgG) against long S-2 region of chicken pectoralis myosin. IgG was added at 1.5 mg/ml. The temperature was 21°C. Upper and lower limits of error envelope indicate extremes of error bars for the goat anti-S-2 antibody and controls, respectively. Solid lines are single exponential fits to averaged data using the fitting routine of Johnson and Frazier (12). See Table 1 for number of runs (*n*) averaged for each data point.

followed by a much slower stage in which the myofibrils undergo further shortening and, within a few seconds, form poorly defined globules characteristic of the supercontracted state. The initial rate (Table 1) of contraction of these (control) myofibrils agrees well with the maximum shortening velocity of glycerinated muscle under zero load (6–7 μm/sec at 15°C) (15).

The initial rate and half-time (Table 1) of shortening of myofibrils in the fast phase in the presence of goat anti-rabbit S-2 are not significantly different from control myofibrils, but the somewhat lower initial rate (70% of control) and longer half-time of the contractile process for myofibrils treated with rabbit anti-chicken S-2 are significant according to Student's *t* test ($P < 0.05$). The reasons for this difference are unclear at present.

At the end of the initial phase of contraction, the averaged sarcomere spacing of antibody-labeled myofibrils is somewhat longer than that of unlabeled myofibrils (Table 1). Unlike control myofibrils, antibody-labeled myofibrils condense into elongated rod-like structures during the subsequent slow phase of contraction and retain well-defined sarcomere spacings (Fig. 2). We estimate the average length of sarcomeres to be about 1 μm (rabbit anti-chicken S-2) after termination of the shortening process.

Previous antibody binding experiments in this laboratory show (unpublished data) that in rigor buffer (pH 7, 4°C), a 1-hr

Table 1. Contraction of rabbit psoas myofibrils (fast phase) in the presence of anti-S-2 antibodies

| Anti-S-2 | *n* | Initial rate, μm/sec | Half-time, msec | $L_o$, μm | $L_f$, μm |
|---|---|---|---|---|---|
| None (control) | 15 | 7.0 ± 1.0 | 129 ± 29 | 2.6 ± 0.1 | 1.3 ± 0.3 |
| Goat antibody | 12 | 6.6 ± 3.5 | 120 ± 34 | 2.7 ± 0.1 | 1.7 ± 0.3 |
| Rabbit antibody | 31 | 4.8 ± 1.5 | 186 ± 48 | 2.7 ± 0.1 | 1.5 ± 0.1 |

Initial rate, half-time, and $L_f$ are averages from exponential fits of separate runs. $L_o$, initial sarcomere length; $L_f$, final sarcomere length. Results are mean ± SD.

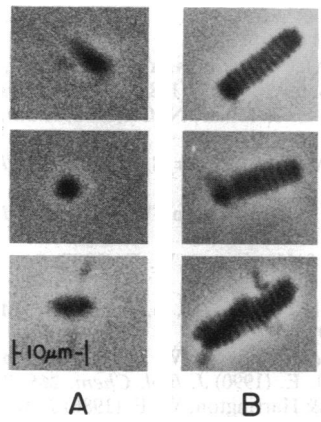


FIG. 2. Myofibrils photographed after completion of slow phase of shortening. (*A*) Control (untreated) myofibrils 20 sec after activation. (*B*) Myofibrils in presence of rabbit anti-chicken S-2 antibody 2.5 min after activation.

incubation is sufficient to saturate anti-S-2 epitopes (three antibodies per myosin) in myofibrils. No difference in antibody binding was observed in these studies under ionic conditions where rigor cross-bridges are released from the thick filament surface [0.05 M, pH 8.5 (16)]. Thus activation of the labeled myofibrils would appear to occur under conditions where the S-2 antibody binding sites are fully saturated.

When single psoas fibers were immersed in activating solutions containing goat anti-rabbit S-2, the isometric force fell rapidly at a rate dependent on the initial concentration of antibody (Fig. 3). At antibody concentrations of 0.5, 1.5, and 4.2 mg/ml, the half-times of force decay were 35 min, 15 min, and ≈0.5 min, respectively, whereas the force generated by untreated (control fibers) decreased at a much slower rate (half-time = 88 min). This result is similar to that observed when isometric psoas fibers are activated in the presence of rabbit anti-chicken S-2 (5). Hence it is clear that the two polyclonal antibodies show comparable behavior in their ability to suppress the isometric force developed in fibers without an appreciable effect on the sliding velocity of myofibrils. Indeed, the inability of the antibody-treated myofibrils to condense into the supercontracted globular state (Fig. 2) may be a consequence of the antibody-induced reduction in sliding force.

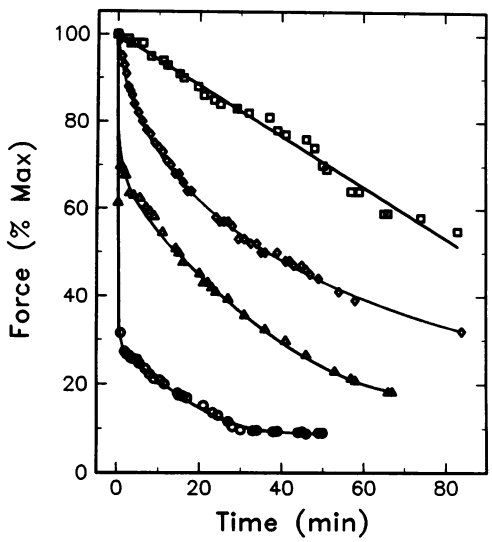


FIG. 3. Decrease in isometric force of activated glycerinated rabbit psoas fibers in the presence of polyclonal goat anti-rabbit S-2 antibody. Antibody was prepared and purified by affinity chromatography as described (5). □, Control; ◇, anti-S-2 at 0.5 mg/ml; △, anti-S-2 at 1.5 mg/ml; ○, anti-S-2 at 4.2 mg/ml. Activating solution was 120 mM NaCl/40 mM cacodylic acid/5.6 mM $MgCl_2$/5 mM $CaCl_2$/2 mM EGTA/2 mM ATP/5 mM creatine phosphate/creatine kinase (0.2 mg/ml), pH 7.2, 10°C.

## DISCUSSION

The main result of this work is that anti-S-2 antibodies reduce the isometric force in muscle fibers but do not inhibit the rate of shortening of myofibrils. The simplest interpretation of this result is that activated S-1 subunits can develop sufficient force to slide actin filaments in an organized unloaded system near maximum velocity, but this process alone is unable to generate the isometric force characteristic of working muscle. Kishino and Yanagida (7) have measured the force developed by a single actin filament interacting with a myosin- or S-1-coated surface, based on the elastic displacement of a thin flexible glass microneedle to which the actin filament is attached. They reported a value of the force per head as 0.2 pN, which was later revised to 0.8 pN as a result of recalibration (17). The maximum force generated per head in a working isometric muscle depends on the fraction of heads attached to actin at any instant in their force-generating state. According to the helix-coil mechanism, it would correspond to those myosin heads that are transiently coupled to melting in the hinge domain of the S-2 segments in a cross-bridge cycle (18). The fraction of heads estimated in the strong-binding rigor-like state, which Huxley and Kress (2) suggest may be the force-generating state, has been reported to be in the range 12–20%, based on steady-state (19–21) and time-resolved (22) EPR studies of actively contracting muscle. By using an independent method (proteolytic digestion), Duong and Reisler (23) also find only a small fraction of myosin heads (25%) form rigor-like bonds during ATP hydrolysis in myofibrils. Calculation (24) shows that the contractile force generated per head by these bridges could be as high as 7–10 pN, assuming the maximum tension (3 kg/cm$^2$) generated by frog muscle fibers (25). We observed in the present and earlier study (5) that the isometric force decreases in the presence of the polyclonal antibody to 5–10% of control rabbit psoas fibers. Hence our results, which suggest that this residual force is contributed primarily by the S-1 subunits attached to actin, are not incompatible with the force measurement of Kishino and Yanagida (7) on isolated myosin heads.

We should also note genetic studies that provide strong supportive evidence that the hinge domain of S-2 has an important physiological role in the contractile process.

Cardiac muscles express only two myosin heavy chain genes that produce the $\alpha$ and $\beta$ heavy chain isoforms (26). The differential expression of the $\alpha$ and $\beta$ myosin heavy chain genes results in heart muscles with markedly different functional properties (myosin containing $\alpha$ heavy chains is a "fast ATPase" myosin that exhibits greater contractile force than myosin containing $\beta$ heavy chains, a "slow ATPase" myosin) (27–29). McNally *et al.* (30) have reported limited and striking sequence differences between $\alpha$ and $\beta$ cardiac myosins including differences in their S-2 hinge domains that, they suggest, could contribute to the differential force produced by $\alpha$- and $\beta$-myosin heavy chains, predominant in heart muscles. One difference cluster is a 29-amino acid segment that lies adjacent to the N terminus of the hinge domain of S-2 (at residues 1076–1104) and the second is a 28-amino acid segment (residues 1249–1276) within the hinge domain.

Myosin heavy chain gene and amino acid sequence studies of *Drosophila* muscle myosin indicate that a part of the S-2 hinge is encoded by two mutually exclusive alternative exons, 15a and 15b. The alternative exons encode 26 residues of the 150-residue S-2 hinge domain (residues 1215–1240) in

the major helix-breaking sequence of this region, as revealed by computer-assisted secondary structure analysis (31). Collier *et al.* (32) have identified the specific defect in a flightless mutant of *Drosophila* (MHC-10) resulting from a mutation within alternative exon 15a. Their work and the work of George *et al.* (31) indicate that *Drosophila* muscles that are required to contract quickly (indirect flight muscle) and/or generate high levels of tension (jump muscles) accumulate transcripts encoding hinge region a, whereas muscles that contract slowly (larval and abdominal muscles of adult) only accumulate hinge region b transcripts. Thus alternative myosin hinges may play an essential role in the generation of different levels of contractile force or shortening speed. We conclude that although the S-1 subunit is capable of movement along actin and can contribute to the generation of contractile force in activated muscle, present evidence implicates the hinge domain as a second site for force generation.

We are grateful to Drs. Michael E. Rodgers and Emil Reisler for helpful discussions. We thank Dr. T. Iwazumi for suggesting the procedure to prepare coverslips. This work was supported by National Institutes of Health Research Grants AR-04349 to W.F.H. and HD-22879 to W.B.B. This is contribution 1456 from the McCollum-Pratt Institute, Department of Biology, The Johns Hopkins University.

1. Huxley, H. E. (1969) *Science* **164,** 1356–1366.
2. Huxley, H. E. & Kress, M. (1985) *J. Muscle Res. Cell Motil.* **6,** 153–161.
3. Harrington, W. F. (1971) *Proc. Natl. Acad. Sci. USA* **68,** 685–689.
4. Harrington, W. F. (1979) *Proc. Natl. Acad. Sci. USA* **76,** 5066–5070.
5. Lovell, S., Karr, T. & Harrington, W. F. (1988) *Proc. Natl. Acad. Sci. USA* **85,** 1849–1853.
6. Harrington, W. F., Rodgers, M. E. & Davis, J. S. (1990) in *Molecular Mechanisms in Muscular Contraction*, ed. Squire, J. M. (Macmillan, New York), pp. 241–263.
7. Kishino, A. & Yanagida, T. (1988) *Nature (London)* **334,** 74–76.
8. Toyoshima, Y. Y., Kron, S. J., McNally, E. M., Niebling, K. R., Toyoshima, C. & Spudich, J. A. (1987) *Nature (London)* **328,** 536–539.
9. Hynes, T. R., Block, S. M., White, B. T. & Spudich, J. A. (1987) *Cell* **48,** 953–963.
10. Somlyo, A. V., Goldman, Y. E., Fujimori, M. B., Trentham, D. R. & Somlyo, A. P. (1988) *J. Gen. Physiol.* **91,** 165–192.
11. Homsher, E. & Millar, N. C. (1990) *Annu. Rev. Physiol.* **52,** 875–896.
12. Johnson, M. L. & Frazier, S. G. (1985) *Methods Enzymol.* **117,** 301–342.
13. Ueno, H. & Harrington, W. F. (1984) *J. Mol. Biol.* **180,** 667–701.
14. Ueno, H. & Harrington, W. F. (1987) *Biochemistry* **26,** 3589–3596.
15. Moss, R. L., Giulian, G. G. & Greaser, M. L. (1983) *J. Cell Biol.* **96,** 970–978.
16. Ueno, H. & Harrington, W. F. (1986) *J. Mol. Biol.* **190,** 59–68.
17. Huxley, H. E. (1990) *J. Biol. Chem.* **265,** 8347–8350.
18. Ueno, H. & Harrington, W. F. (1986) *J. Mol. Biol.* **190,** 69–82.
19. Cooke, R., Crowder, M. S. & Thomas, D. D. (1982) *Nature (London)* **300,** 776–778.
20. Cooke, R., Crowder, M. S., Wendt, C. H., Barnett, V. A. & Thomas, D. D. (1984) in *Contractile Mechanisms in Muscle*, eds. Pollack, G. H. & Sugi, H. (Plenum, New York), pp. 413–423.
21. Barnett, V. A. & Thomas, D. D. (1989) *Biophys. J.* **56,** 517–523.
22. Fajer, P. G., Fajer, E. A. & Thomas, D. D. (1990) *Proc. Natl. Acad. Sci. USA* **87,** 5538–5542.
23. Duong, A. M. & Reisler, E. (1989) *Biochemistry* **28,** 1307–1313.
24. Squire, J. M. (1986) *Muscle Design, Diversity and Disease* (Benjamin, Reading, MA), p. 275.
25. Huxley, A. F. & Simmons, R. M. (1971) *Nature (London)* **233,** 533–538.
26. Mahdavi, V., Chambers, A. P. & Nadal-Ginard, B. (1984) *Proc. Natl. Acad. Sci. USA* **81,** 2626–2630.
27. Schwartz, K., Lecarpentier, Y., Martin, J. L., Compre, A. M., Mercardier, J. J. & Swynghedauw, B. (1981) *J. Mol. Cell. Cardiol.* **13,** 1071–1075.
28. Morano, I., Arndt, H., Gartner, C. & Caspar-Ruegg, J. (1988) *Circ. Res.* **62,** 632–639.
29. Pope, B., Hoh, J. F. Y. & Weeds, A. (1980) *FEBS Lett.* **118,** 205–211.
30. McNally, E. M., Kraft, R., Bravo-Zehnder, M., Taylor, D. A. & Leinwand, L. A. (1989) *J. Mol. Biol.* **210,** 665–671.
31. George, E. L., Ober, M. B. & Emerson, C. P., Jr. (1989) *Mol. Cell. Biol.* **9,** 2957–2974.
32. Collier, V. L., Kronert, W. A., O'Donnell, P. T., Edwards, K. A. & Bernstein, S. I. (1990) *Genes Dev.* **4,** 885–895.